Oct 23rd, 12:00 AM

Stainless Steel Tubular Columns - Tests and Design

Gregory J. Hancock

Kim J. R. Rasmussen

Tenth International Specialty Conference on Cold-formed Steel Structures
St. Louis, Missouri, U.S.A., October 23-24, 1990

STAINLESS STEEL TUBULAR COLUMNS - TESTS AND DESIGN

by

Kim J.R. Rasmussen[1] and Gregory J. Hancock[2]

Summary

The paper presents tests on square and circular section stainless steel tubes, including stub column and long column tests. The tests focus on the increase in strength resulting from cold-work during the fabrication process. Tension and compression tests on coupons cut from finished tubes are also included in the paper, as are measurements of residual strains produced by the cold-rolling process.

A design procedure is proposed for stainless steel tubular columns based on the tests. It is demonstrated that the proposed design procedure provides column strengths which are much closer to the test strengths than design strengths based on the annealed material properties.

1 Lecturer, School of Civil and Mining Engineering,
University of Sydney, NSW 2006, Australia

2 Associate Professor, School of Civil and Mining Engineering,
University of Sydney, NSW 2006, Australia

1 Introduction

The paper describes tests on stainless steel sections cold-formed and welded to produce tubular sections. The purpose of the tests was to determine the compressive strength of stainless steel structural hollow sections and to develop guidelines for the design of these sections as structural members.

A design method for stainless steel structural members was given in the 1968 AISI Stainless Steel Cold-Formed Structural Design Manual (AISI 1968a), which was based mainly on the 1968 AISI Specification for the Design of Cold-Formed Steel Structural Members (AISI 1968b) but modified for the particular characteristics of stainless steel material. These characteristics include a rounded stress-strain curve for stainless steel which is different from that for cold-formed carbon steel, and which is different in tension and compression. A revision of the 1968 stainless steel specification was published in 1974 (AISI 1974). In 1986, the AISI produced a major revision (AISI 1986) of its specification for cold-formed carbon steel members, which required a revision of the 1974 Specification for Stainless Steel Members. This was produced at the University of Missouri-Rolla as the Proposed Specification for the Design of Cold-Formed Stainless Steel Structural Members (University of Missouri Rolla, Civil Engineering Study 88-1 (CES 88-1), 1988).

The proposed specification (CES 88-1) is based on the stress-strain characteristics of the annealed (or strain flattened) stainless steel strip. However, the process of forming an annealed strip into a tubular section by cold-working and welding produces considerable enhancement of the stress-strain characteristics of the annealed steel. This process is well known for carbon steel tube and has been allowed for in the American Specification ASTM A500-84 (ASTM 1984) for structural hollow sections cold-formed from carbon steel. In this case, the tensile and yield strengths determined for the formed tube are allowed to be used in design according to the American Steel Structures Specification (AISC 1986) and the American Cold-Formed Steel Structures Specification (AISI 1986).

It is the purpose of this paper to determine whether the stress-strain characteristics of stainless steel tube determined after cold-forming can be used in the structural design of stainless steel tubular columns. Since the square hollow section undergoes a different amount of cold-work from the circular hollow sections, the stress-strain characteristics for stainless steel square hollow sections will be different from those for stainless steel circular hollow sections. The difference is determined as part of the test programme described in the paper.

2 Test Programme

2.1 Outline of the test programme

The tests were performed on tubes of austenitic stainless steel of type 304L, having a Nickel content between 8 and 13 %, a Chrome content between 18 and 20 %, and a maximum Carbon content of 0.035 %. The tubes were cold-rolled from annealed flat strips which had been rolled on coils. The test programme included stub column tests and long column tests of the nominal 80×3.0 square hollow section (SHS) and the nominal 101.6×2.85 circular hollow section (CHS).

The stub column tests were performed to determine the 0.2 % Proof Stress ($\sigma_{0.2}$) and the variation of the tangent modulus ($E_t = d\sigma/d\varepsilon$) with the stress. The long column tests were performed at three or four lengths to determine the reduction of column strength with increasing column length. Two tests were performed for each column length. In the first test, the axial load was applied at the geometric centroid to allow determination of the ultimate load of a concentrically loaded column. In the second test, the load was applied with a nominal eccentricity relative to the geometric centroid equal to one thousandth of the length. The second test was performed to determine the ultimate load of an imperfect column.

Tets coupons were cut from an 80×3.0 SHS tube and a 101.6×2.85 CHS tube to determine the stress-strain curves of the material in its cold-worked state. Both compression and tension coupon tests were performed, as described in Section 2.5.

Substantial residual strains are introduced during the cold-rolling process. These residual strains were measured for an 80×3.0 SHS tube and a 101.6×2.85 CHS tube, as described in Section 2.6.

The test specimens have been labelled so that the section type (SHS or CHS), the type of test, and the loading eccentricity details can be identified from the label, as demonstrated in Fig. 1. The first two symbols of the label are either S1 or C1 denoting an SHS or CHS respectively. The subsequent letter(s) are either SC or L denoting a stub column (SC) or a long column (L) test specimen. If it is a stub column test specimen, the SC is followed by an identification number, 1 or 2. If it is a long column test specimen, the L is followed by the specimen length in mm and then by either a C or an E, denoting a concentrically loaded (C) or an eccentrically loaded (E) test specimen.

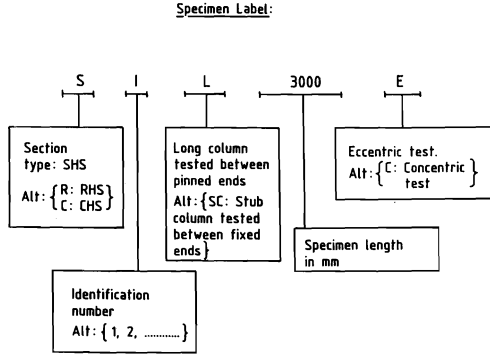

Figure 1: Specimen labelling system

2.2 Stub column tests

The measured cross-section dimensions and the measured specimen length of the stub column test specimens are given in Tables 1a and 1b for the SHS and CHS respectively. The symbols used in Table 1 are defined in Fig. 2.

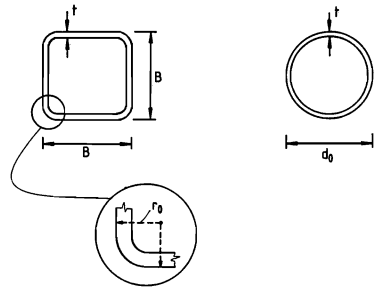

Figure 2: Section Geometry

The stub columns S1SC2 and C1SC2 were instrumented with four and three longitudinal strain-gauges respectively located at midlength. The stub columns were tested using a vertical DARTEC test rig by applying the loading using a servo-controlled 2000 kN capacity hydraulic ram. The specimen was supported on rigid platens, the bottom platen being fixed against rotation, and the top platen mounted on a spherical seat to allow full contact between the test specimen and the end platens.

Stress-strain curves for the complete cross-section in the cold-worked state were obtained for the S1SC2 and C1SC2 stub columns, as shown in Figs. 3a and 3b respectively. In the figures, the strain (ε) is the average of the strain gauge readings and the stress (σ) is the load (P) divided by the area (A) calculated using the measured cross-section dimensions given in Table 1. Figures 3a and 3b also include the initial Young's modulus (E_0), determined by fitting a straight line through the stress-strain curves in the linear range of material behaviour. These initial moduli were $E_0 = 191$ GPa and $E_0 = 201$ GPa for the SHS and the CHS respectively.

As preparation for the determination of long column strengths, modified Ramberg-Osgood curves (Ramberg & Osgood 1943, Hill 1944) were fitted through the measured stress-strain curves. The modified Ramberg-Osgood curve is expressed in the form,

$$\varepsilon = \frac{\sigma}{E_0} + 0.002(\frac{\sigma}{\sigma_{0.2}})^n \tag{1}$$

where E_0 is the initial Young's modulus, $\sigma_{0.2}$ is the 0.2 % Proof Stress and n is a positive constant. The values of the quantities $(E_0, \sigma_{0.2}, n)$ are given in Table 2 for the SHS and CHS stub columns. The modified Ramberg-Osgood stress-strain curves are included in Fig. 3 to provide comparison with the test curves obtained for the S1SC2 and C1SC2 stub columns.

2.3 Tangent modulus versus stress curves

The tangent modulus ($E_t = d\sigma/d\varepsilon$) is required to determine the behaviour and strength of the long columns. It was obtained as a function of the stress (σ) for the SHS and CHS by taking the derivative of the modified Ramberg-Osgood stress-strain curves given by

Specimen	B	t	r_o	v_{01}	e_{01}	$\lvert v_{01}-e_{01}\rvert/L_t$	v_{02}	e_{02}	$\lvert v_{02}-e_{02}\rvert/L_t$	L	L_t/r	P_u
	(mm)						(mm)			(mm)	(Note 1)	(kN)
S1SC1	80.4	3.00	5.5	–	–	–	–	–	–	300	5	485
S1SC2	79.7	3.00	5.5	–	–	–	–	–	–	298	5	471
S1L1000C	80.5	2.90	6.0	0.3	−0.4	1/2070	0.2	0.2	0	1001	46	390
S1L1000E	80.3	2.98	5.0	0.6	−0.3	1/1610	−0.3	0.2	1/2900	1001	46	344
S1L2000C	80.4	2.99	6.0	0.1	−0.5	1/4080	0.1	0.7	1/4080	2000	79	193
S1L2000E	80.6	2.93	6.0	0.7	−3.4	1/600	−0.3	0.6	1/2720	2000	79	158
S1L3000C	80.7	2.95	5.5	1.6	−0.5	1/1640	−1.1	0.4	1/2300	3002	111	96
S1L3000E	80.2	2.98	5.5	2.1	−3.2	1/650	−0.2	0.3	1/6900	3001	111	98
Mean	80.4	2.97	5.5									
S.D. (Note 2)	0.3	0.04	0.4									

Note 1: Nominal value of r. L_t includes the end bearing dimension (450 mm) and is half of the constructed length for the fixed-ended stub column tests.
Note 2: Standard Deviation.

a) SHS

Specimen	d_o	t	v_{01}	e_{01}	$\lvert v_{01}-e_{01}\rvert/L_t$	v_{02}	e_{02}	$\lvert v_{02}-e_{02}\rvert/L_t$	L	L_t/r	P_u
	(mm)					(mm)			(mm)		(kN)
C1SC1	101.6	2.96	–	–	–	–	–	–	350	5	426
C1SC2	101.6	2.96	–	–	–	–	–	–	350	5	425
C1L1000C	101.4	2.98	0.1	0.6	1/2900	0.2	−0.4	1/2420	1000	42	328
C1L1000E	101.5	2.98	0.2	−1.7	1/760	0.2	0.2	0	1001	42	303
C1L2000C	101.5	2.95	0.3	0.3	0	0.0	−0.1	1/24500	2000	70	241
C1L2000E	101.4	2.92	0.7	−1.4	1/1170	0.1	0.6	1/4900	2001	70	198
C1L3000C	101.4	2.93	0.7	1.0	1/11500	0.3	0.6	1/11500	3000	99	171
C1L3000E	101.4	2.93	1.2	−2.4	1/960	0.6	0.6	0	3000	99	127
C1L4000C	101.3	2.96	1.5	1.3	1/22250	0.7	1.7	1/4450	4000	127	113
C1L4000E	101.3	2.93	2.0	−4.1	1/730	1.2	2.5	1/3420	4000	127	84
Mean	101.4	2.95									
S.D.	0.1	0.02									

b) CHS

Table 1: Dimensions, geometric imperfections, loading eccentricities and ultimate loads of SHS and CHS test specimens.

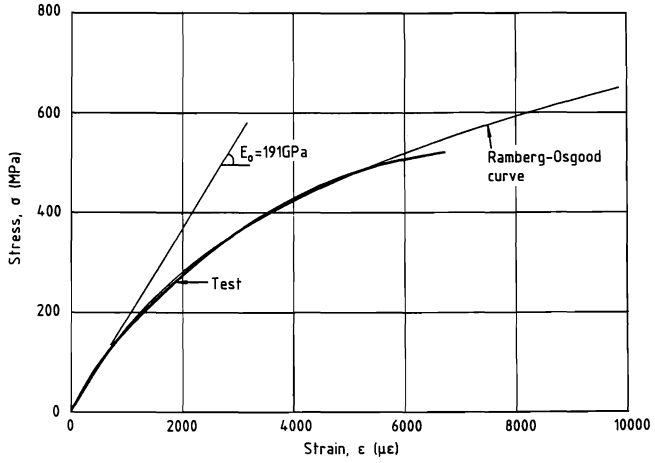

a) S1SC2

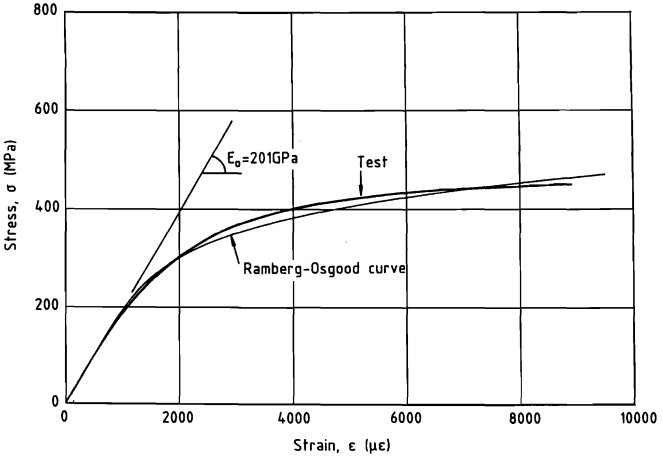

b) C1SC2

Figure 3: Stress-strain curves for the total cross-sections of SHS and CHS stub columns.

Section type	E_0 (GPa)	$\sigma_{0.2}$ (MPa)	n
SHS	191	440	3.0
CHS	201	380	6.0

Table 2: Ramberg-Osgood parameters for stress-strain curves of SHS and CHS stub columns.

eqn. (1). Accordingly, the tangent modulus was expressed as,

$$E_t = \frac{\sigma_{0.2}\, E_0}{\sigma_{0.2} + 0.002\, n\, E_0 \left(\frac{\sigma}{\sigma_{0.2}}\right)^{n-1}} \tag{2}$$

The tangent modulus versus stress curves are shown in Fig. 4, for the SHS and CHS. The curves were produced using eqn. (2) by substituting the values of E_0, $\sigma_{0.2}$ and n given in Table 2. The SHS has lower values of E_t than the CHS at lower stress levels and higher values of E_t at higher stress levels. This is a consequence of the greater amount of cold-work required to produce an SHS than a CHS.

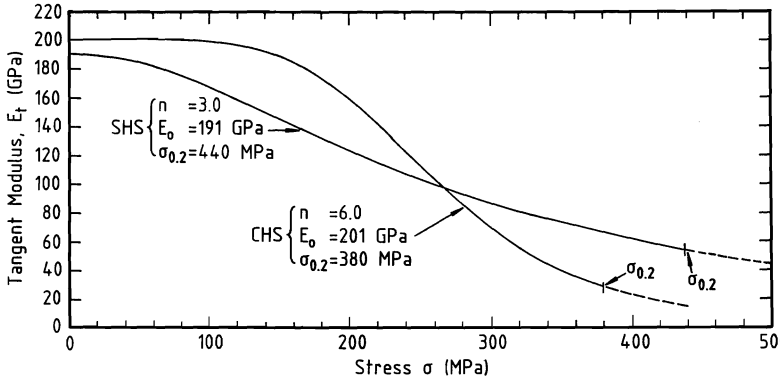

Figure 4: Tangent modulus versus stress curves for SHS and CHS.

2.4 Long column tests

The SHS long column test specimens and the stub columns, S1SC1 and S1SC2, were produced from the same coil and so were expected to have nearly identical material properties. Similarly, the CHS long column test specimens and the stub columns, C1SC1 and C1SC2, were produced from the same coil and so were expected to have nearly identical material properties.

The SHS long columns were tested at three lengths corresponding to specimen lengths (L) of 1000 mm, 2000 mm and 3000 mm. The CHS long columns were tested at four lengths corresponding to specimen lengths of 1000 mm, 2000 mm, 3000 mm and 4000 mm. The

column length ($L_t = L + 2L_b$), measured as the distance between the axes of the pinned end bearings of the testing rig, was equal to the sum of the specimen length (L) and the dimensions of the end bearings (L_b=225 mm). Therefore, the SHS long columns were tested at column slenderness (L_t/r) values equal to 46, 79 and 111, where r=31.2 mm is the radius of gyration of the nominal 80×3.0 SHS. Similarly, using a value of the radius of gyration for the nominal 101.6×2.85 CHS equal to 34.9 mm, the CHS long columns were tested at column slenderness values equal to 42, 70, 99 and 127. The measured cross-section dimensions and specimen lengths of the SHS and CHS long columns are given in Tables 1a and 1b respectively. The symbols defining the cross-section dimensions in Table 1 are explained in Fig. 2.

The ends of the test columns were milled flat to within 0.002 mm to allow proper seating on the end-platens of the testing rig. Subsequently, four linear strain gauges were attached longitudinally to the specimens at midlength. For the SHS columns, the gauges were placed at the centre of each flat face. For the CHS columns, the gauges were placed at 90° angles measured circumferentially such that two of the gauges were located in the plane in which the column had the largest overall imperfection (deviation of the column axis from a straight line).

The geometric imperfections of the SHS and CHS long columns were measured at midlength before testing. The imperfections of the SHS columns were obtained by stretching a thin metal wire between the ends and recording the distance from the wire to the specimen at midlength. The readings were taken in a horizontal plane to eliminate gravity effects. The imperfections were measured in both principal directions and are given as v_{01} and v_{02} in Table 1a. The geometric imperfections of the CHS long columns were measured using a Wild NA2 optical level and a GPM3 parallel plate optical level. The imperfection measurements at midlength in the principal directions are given as v_{01} and v_{02} in Table 1b, where the principal directions are defined as the plane with the largest geometric imperfection and the plane perpendicular to this. Using the values of v_{01} and v_{02} in Table 1, the maximum relative imperfections ($\max\{v_{01}/L_t, v_{02}/L_t\}$) of the SHS and CHS long columns were obtained as 1/1640 and 1/2230 respectively.

Local plate imperfections were not measured on the SHS and CHS long columns. It was observed that there was no discernible out-of-flatness of the faces of the SHS along the length of the columns.

Two tests were performed for each column length. The first test (labelled with a C as the last symbol in the test specimen label) was to determine the strength of a concentrically loaded specimen with the line of action of the applied load based on the geometric centroid of the cross-section. The second test (labelled with an E as the last symbol in the test specimen label) was to determine the strength of an imperfect column. Because the *average* measured geometric imperfection (average of $\max\{v_{01}, v_{02}\}$) was equal to $L_t/3030$ and $L_t/3960$ for the SHS and CHS long columns respectively, end loading eccentricities (e_{01}, e_{02}) in the principal directions were incorporated into the tests. At stresses in the linear range of material behaviour, readings measuring the longitudinal strain and the lateral deflections in the principal directions were used to calculate the eccentricities of the line of action of the external force relative to the position of the geometric centroid at the end sections. The results are given as e_{01} and e_{02} in Table 1. The distance from the line of action of the external force to the geometric centroid of the specimens at midlength is given by $|v_{01} - e_{01}|$ and $|v_{02} - e_{02}|$. These distances are given relative to the column length (L_t) in Table 1.

The tests determining the strength of imperfect columns were performed using a nominal eccentricity of a thousandth of the pinned column length. As shown in Table 1, the measured relative eccentricities ($|v_{01} - e_{01}|/L_t$) of the eccentrically loaded SHS and CHS specimens varied between 1/1610 and 1/600. This variability reflects the difficulty of positioning a specimen in the test rig at a certain eccentricity relative to the line of action of the external force.

The long columns were tested between pinned ends using a 2000 kN capacity DARTEC servo-controlled hydraulic ram in a horizontal reaction frame. The loading was applied to the specimen by rigid end platens mounted on bearings which were free to rotate about both principal axes of the cross-section. The measured ultimate loads (P_u) of the long columns are given in Table 1. Local buckling, causing distortions of the cross-section, was not observed in the SHS and CHS long column tests, except in the tests of the specimens S1L1000C and S1L1000E which formed inelastic local buckles at midlength in the face with the greatest compressive strain at advanced stages of post-ultimate loading.

2.5 Tension and compression coupon tests

Tension and compression coupons were cut from SHS and CHS tubes belonging to the same batches as the SHS and CHS stub columns and long columns at the positions shown in Fig. 5. The figure also shows the labelling of the coupons and their widths, measured as the narrowest widths between the parallel sides. The tension coupon dimensions conformed to the Australian Standard AS1391 (SAA 1974) for the tensile testing of metals.

The compression coupons were tested using a bracing jig. The bolts containing the coupons within the jig were sufficiently tight to prevent lateral buckling, yet sufficiently loose to allow unrestrained Poisson expansion. Also, to reduce friction between test coupon and jig, the contact surfaces were smeared with a thin layer of lubricating paste before assembly.

Each tension and compression coupon was instrumented with two linear strain gauges. The gauges on coupons cut from the flat parts of the SHS and from the CHS were placed so that the average of the two strain readings provided the longitudinal strain at the geometric centroid of the coupon. The strain gauges allowed determination of the initial Young's modulus ($E_0 = d\sigma/d\varepsilon\,|_{\sigma=0}$) and the 0.2 % Proof Stress.

The tension and compression coupons curved longitudinally after being cut from the tube because of large through-thickness bending residual stresses, as described in Section 2.6. However, while tightening the ends of the tension coupons in the friction grips the coupons straightened and almost returned to their flat state. Consequently, the longitudinal through-thickness bending residual stresses present in the finished tube were approximately reintroduced in the tension coupons during gripping. Likewise, the compression coupons were straightened and became nearly flat as the bolts of the bracing jig were tightened before testing. This process should also have reintroduced approximately the longitudinal through-thickness bending residual stresses present in the finished tube.

The coupons were tested in accordance with AS1391 (SAA 1974) using a low strain rate ($< 15\mu\varepsilon$/s) at strains less than 20 000 $\mu\varepsilon$. At strains greater than 20 000$\mu\varepsilon$, the strain

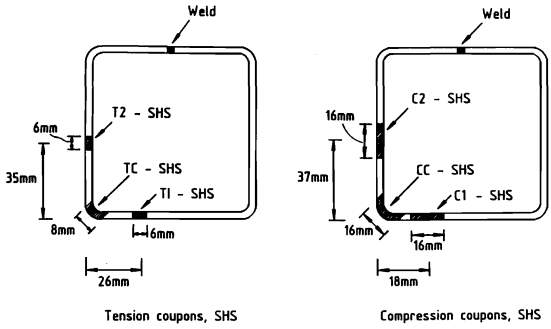

a) SHS

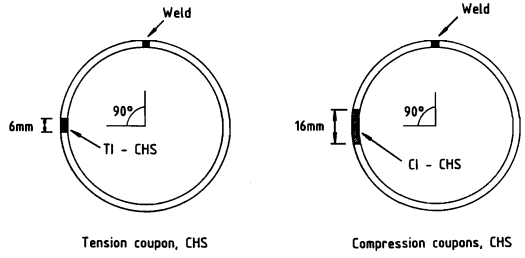

b) CHS

Figure 5: Location of tension and compression test coupons in cross-section.

rate of the tensile coupons was increased to approximately 5 000 $\mu\varepsilon$/s. The ultimate tensile strength (σ_u) was measured near the conclusion of the test after pausing the applied straining for one minute.

Readings of the load and the two strain gauges were taken at regular intervals during the tests using a Spectra MS-208 data acquisition system which was controlled by a micro computer. The stress-strain curves obtained from the tension and compression coupon tests are shown in Figs. 6 and 7 for the SHS and CHS respectively. In the figures, the strain (ε) is the average of the two strain gauge readings and the stress (σ) is the measured load divided by the initial area calculated using the coupon dimensions measured before testing. As shown in Figs. 6 and 7, the scale on the strain axis changes at 20 000 $\mu\varepsilon$. This was also the strain at which the strain rate was increased in the tests.

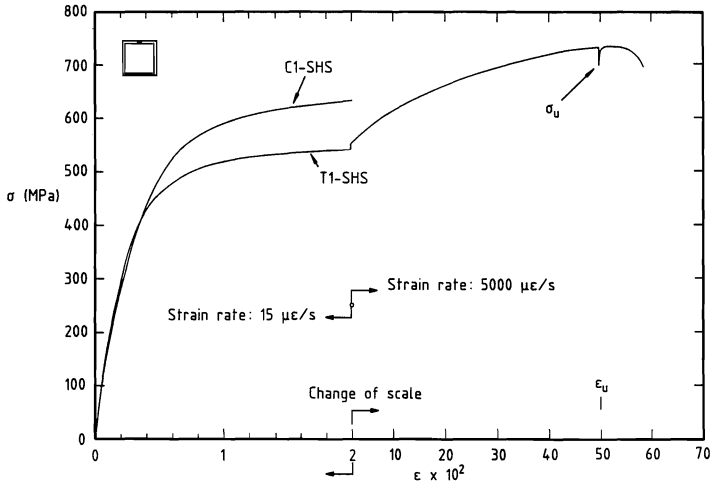

a) T1-SHS and C1-SHS coupons

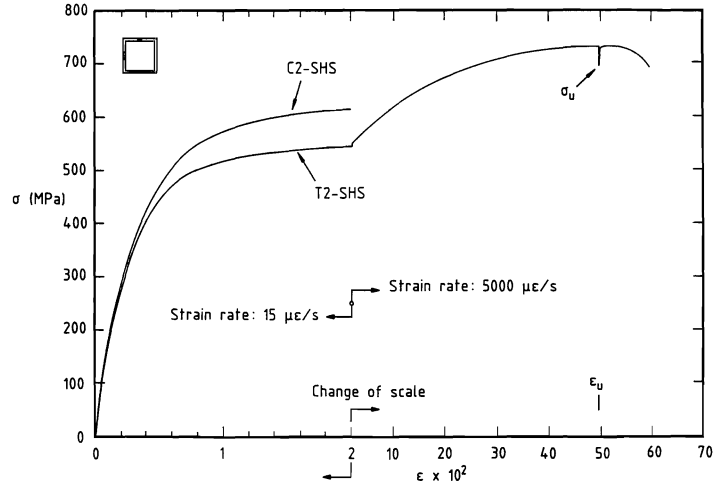

b) T2-SHS and C2-SHS coupons

Figure 6: Tension and compression stress-strain curves for SHS.

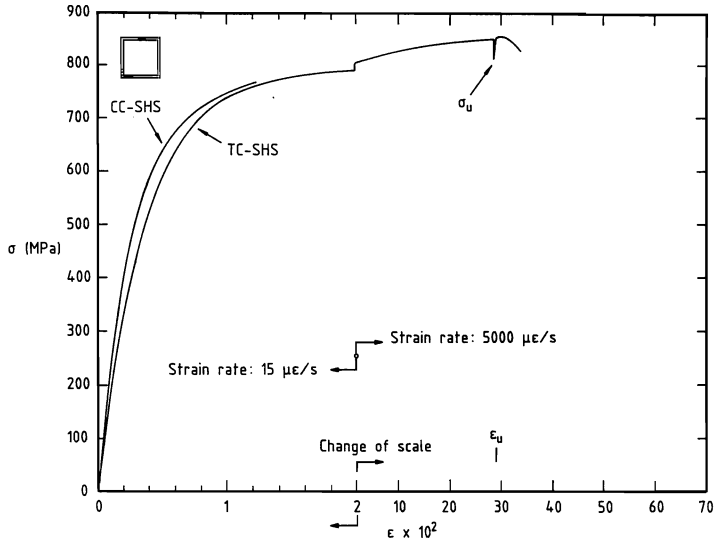

c) TC-SHS and CC-SHS coupons

Figure 6 (continued): Tension and compression stress-strain curves for SHS.

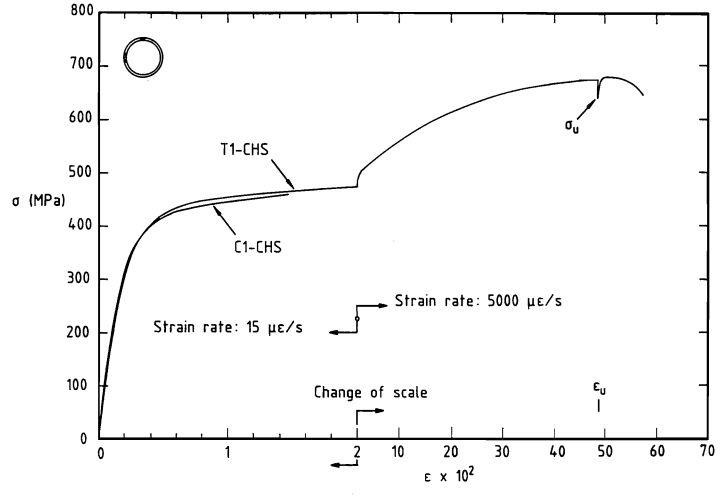

Figure 7: Tension and compression stress-strain curves for CHS.

Figures 6a and 6b show the stress-strain curves for tension and compression coupons cut at different locations of the flat faces of the SHS, as shown in Fig. 5a. For both locations, the stress-strain curve for compression is higher than that for tension at strains greater than 2 000 $\mu\varepsilon$. The stress-strain curves for the T1-SHS and C1-SHS coupons cross over at approximately 1800 $\mu\varepsilon$, and the material is initially stiffer in tension than in compression, as shown in Fig. 6a. However, this result was not obtained in the tests of the T2-SHS and C2-SHS coupons for which the tensile stress-strain curve was lower than the compressive throughout the tests, as shown in Fig. 6b. The tensile strain (ε_u) of the flat faces corresponding to the ultimate tensile strength (σ_u) was approximately 50 % as shown in Figs. 6a and 6b, indicating a very ductile material behaviour of the flat parts of the SHS.

The tensile and compressive stress-strain curves for the corner coupons of the SHS are shown in Fig. 6c. The stress-strain curves are significantly higher than for the flat parts of the cross-section (Figs. 6a and 6b) as a result of the increased cold-work of the corner areas. The ultimate tensile strength (σ_u) is also higher than for the flat parts of the cross-section. However, the corresponding tensile strain (ε_u) is reduced from approximately 50 % for the flat parts to approximately 30 %. The tensile stress-strain curve for the corner areas is lower than the compressive stress-strain curve, as shown in Fig. 6c. However, for the corner coupons it was not possible to attach the strain gauges at equal distances from the neutral axis. Consequently, the bending, which occurred during initial loading as a result of the curvature produced by bending residual stresses, may have influenced the initial part of the stress-strain curves.

Figure 7 shows the tensile and compressive stress-strain curves of the T1-CHS and C1-CHS coupons which were cut from the CHS as shown in Fig. 5b. The stress-strain curves are generally close. They cross over and the tensile curve is higher than the compressive at strains greater than 1700 $\mu\varepsilon$. This result is in contrast to the SHS section coupon tests in which the material showed greater strength in compression than in tension at large strains, as shown in Figs. 6a and 6b.

The difference between the tensile and compressive stress-strain curves for the SHS and CHS reflects the different cold-forming processes of the two sections. The effect of the additional cold-work of the SHS is to raise the stress-strain curves and increase the difference between the tensile and compressive stress-strain curves when compared to the CHS.

The initial Young's modulus (E_0), the 0.2 % Proof Stress ($\sigma_{0.2}$) and the ultimate tensile strength (σ_u) have been determined from the coupon tests and are given in Table 3. The table also includes the tensile strain (ε_u) corresponding to the ultimate tensile strength as shown in Figs. 6 and 7.

2.6 Residual strains

The longitudinal membrane and bending residual strains were measured using strain gauges for SHS and CHS tubes belonging to the same batches as the stub column and long column test specimens. The strain gauges were attached to both the outer and inner surfaces away from the weld line. For the SHS, the gauges were attached at the centre of a flat face. Readings were taken before and after slicing the tubes to provide the released residual strains at the surfaces. The measured strains are shown in Tables 4a

Coupon	E_0	$\sigma_{0.2}$	σ_u	ε_u
	(GPa)	(MPa)		(%)
T1-SHS	194	420	695	49.6
T2-SHS	194	395	695	49.5
TC-SHS	(190)*	580	805	29.0
C1-SHS	195	420	-	-
C2-SHS	197	410	-	-
CC-SHS	(213)	645	-	-
T1-CHS	198	390	640	48.5
C1-CHS	202	390	-	-

( )* The value of E_0 may be affected by initial bending of the coupon.

Table 3: Tension and compression coupon test results for SHS and CHS.

and 4b for the SHS and CHS respectively.

The *membrane* residual strains were obtained by averaging the released strains measured at opposite surfaces, and are given in Table 4. As shown in the table, the membrane residual strains of the SHS and CHS sections were negligible. However, the *bending* residual strains of the CHS and the flat faces of the SHS, calculated as the difference between the measured residual strains at opposite surfaces, were considerable. As shown in Table 4, the bending residual strains for the SHS and CHS were equal to $6237\mu\varepsilon$ and $1594\mu\varepsilon$ respectively. Thus, the bending residual strain of the flats of the SHS was greater than the bending residual strain of the CHS. This result is consistent with the different rolling processes of the two cross-sections: The SHS is first shaped into a circular tube before proceeding through a second set of rollers which flattens the faces and creates a square cross-section. Thus, the SHS is more heavily worked than the CHS and is therefore expected to have higher residual strains. This result is also confirmed by comparing the stress-strain curves of the stub columns S1SC2 and C1SC2 shown in Figs. 3a and 3b respectively, and the stress-strain curves from the coupon tests shown in Figs. 6 and 7, for which the effect of higher residual stresses is to cause earlier yielding and hence earlier departure from linearity in the SHS than in the CHS.

3 Design recommendations for stainless steel tubular columns

3.1 General

The buckling load of a straight concentrically loaded column in the nonlinear range of material behaviour is frequently calculated using the tangent modulus theory or the reduced modulus theory. Generally, the latter theory slightly overestimates the column buckling strength while the former theory tends to underestimate the strength, particularly in the low column slenderness range.

According to the tangent modulus theory, a straight concentrically loaded column buck-

Strain gauge	Initial reading	Reading after slicing	Residual strain*	Membrane residual strain	Bending residual strain
			($\mu\varepsilon$)		
Outer surface	7470	4333	3137	19	6237
Inner surface	7170	10270	−3100		

* Residual strains positive as tensile

a) SHS

Strain gauge	Initial reading	Reading after slicing	Residual strain	Membrane residual strain	Bending residual strain
			($\mu\varepsilon$)		
Outer surface	17940	17149	791	−6	1594
Inner surface	16835	17638	−803		

b) CHS

Table 4: Residual strain measurements of SHS and CHS.

les in an overall mode when the stress equals the critical value,

$$\sigma_{cr} = \frac{\pi^2 E_t r^2}{L_e^2} \tag{3}$$

where $r = \sqrt{I/A}$ is the radius of gyration, $E_t = d\sigma/d\varepsilon$ is the tangent modulus at the stress σ_{cr}, and L_e is the effective column length.

Barlow (1941), Johnson & Winter (1966) and Johnson (1967) determined the tangent modulus of stainless steel columns by testing stub columns and deriving the modulus from the stress-strain curves for the total cross-sections. The approach accounted correctly for variations of the tangent modulus around the cross-section in respect of axial rigidity (E_tA). However, it could overestimate the flexural rigidity (E_tI) when areas having stiffer material were located near the bending axis.

For the SHS tubes, the highly worked corner areas have higher stiffness than the flat parts of the cross-sections, as described in Section 2.5. Since the corner areas are located nearly at the maximum distance from the bending axis, it is expected that using the stress-strain curve for the total cross-section to determine the flexural rigidity (E_tI) will produce conservative predictions of the buckling strength for the SHS.

3.2 Proposed design procedure

It is proposed that the tested SHS and CHS stainless steel tubular columns be designed in accordance with the Proposed Specification, 'Design of Cold-formed Stainless Steel Structural Members', (University of Missouri Rolla, Civil Engineering Study 88-1 (CES 88-1), 1988), with the modifications listed below.

According to Section 3.4 of the CES 88-1, the flexural buckling load (P_a) of a compact column shall be calculated as,

$$P_a = \frac{A F_n}{\Omega} \tag{4}$$

In this equation, Ω is a factor of safety and F_n is the flexural buckling stress determined as,

$$F_n = \frac{\pi^2 E_t r^2}{L_e^2} \leq F_y \tag{5}$$

where F_y is the compressive yield stress. According to CES 88-1, the tangent modulus (E_t) shall be determined using Tables A13 and A14 or Figs. A11 and A12 of the same document. Thus for tubes formed from annealed strips, the appropriate curves to be used in Figs. A11 and A12 would be those for annealed sections. *However, it is proposed here that the column strength of the SHS and CHS columns be determined using eqns. (4,5) with the tangent modulus calculated on the basis of the stress-strain curves obtained from tests of stub columns in the cold-worked state. The stress-strain curves are those which were expressed as modified Ramberg-Osgood curves and defined by eqn. (1) in conjunction with the parameters given in Table 2.*

Section 6.4 of CES 88-1 allows the compressive yield stress (F_y) to be determined by means of a stub column test, with the compressive yield stress taken as either the maximum compressive strength of the section or the 0.2 % Proof Stress ($\sigma_{0.2}$) whichever is reached first in the test. *It is proposed here that the yield stress (F_y) used in eqn. (5) be taken as the Proof Stress ($\sigma_{0.2}$) given in Table 2.* This proposal is made because the ultimate strength of the SHS and CHS stub columns exceeded the 0.2 % Proof Stress.

3.3 Comparison of proposed design strength with test

3.3.1 Design strength curve

The predictions obtained from the modified design procedure proposed in Section 3.2 for the SHS and CHS stainless steel columns are compared with the test strengths in Figs. 8a and 8b respectively. In the figures, the strength curves are calculated for the average dimensions of the SHS and CHS sections given in Tables 1a and 1b respectively, using a factor of safety (Ω) equal to unity. The curves were obtained iteratively using the tangent modulus versus stress curves given in Fig. 4. However, according to eqn. (5) the design stress was limited at the yield stress value (F_y), equal to the 0.2 % Proof Stresses given in Table 2. The hollow and filled circular markers in Figs. 8a and 8b are the test strengths of the concentrically and eccentrically loaded tests respectively, and the hollow square markers are the results of the stub column tests of the SHS and CHS sections. The Euler curves shown in Figs. 8a and 8b are based on values of Young's modulus equal to the measured initial modulus (E_0) of the SHS and CHS sections.

The design philosophy in CES 88-1 is based on columns assumed to be straight and concentrically loaded. Hence, the design curves are to be compared with the test strengths of the concentrically loaded test specimens. As shown in Figs. 8a and 8b, the shapes of the proposed design strength curves agree fairly well with the test strengths of the concentrically loaded specimens although the test strengths are higher than the design curves, except for the specimen S1L3000C. (The strength of this specimen was also less

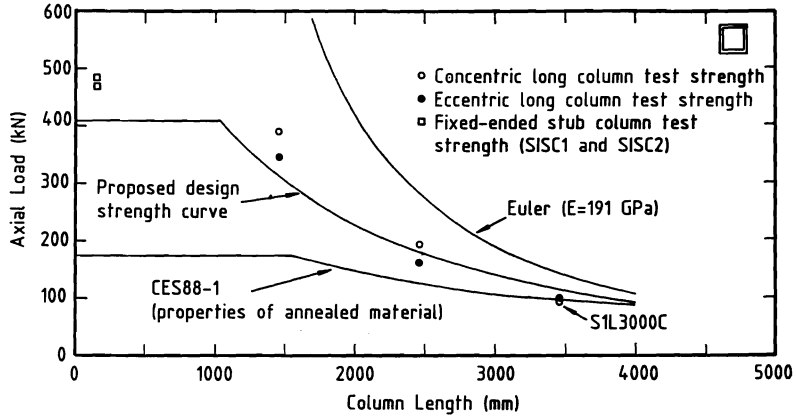

a) SHS

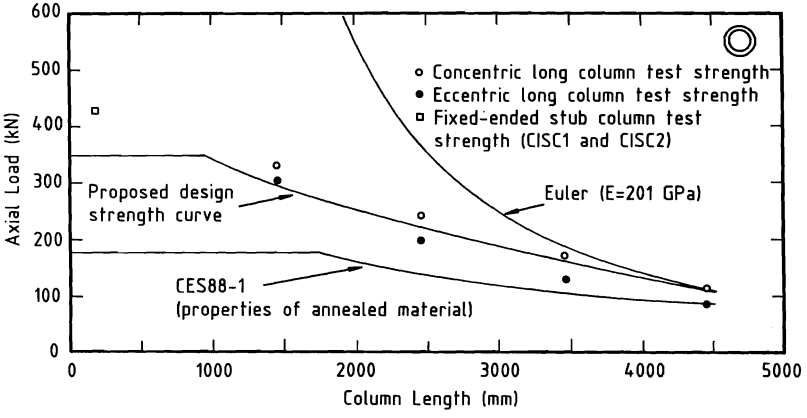

b) CHS

Figure 8: Comparison of proposed design procedure with test strengths.

than the strength of the nominally identical eccentrically loaded specimen S1L3000E. The low strength of the test specimen S1L3000C is attributed to the relatively large initial imperfections in both the principal directions ($|v_{01} - e_{01}|/L_t = 1/1640$ and $|v_{02} - e_{02}|/L_t = 1/2300$ as shown in Table 1a), which induced deflections in both principal directions from the onset of loading, causing failure in a state of biaxial bending at a reduced ultimate load).

It appears from Figs. 8a and 8b, that the strengths of the concentrically loaded test specimens are more conservatively predicted by eqns. (4,5) in the low column slenderness range. This observation is generally supported by the tangent modulus theory (Bild & Trahair, 1988).

Figure 8 also includes the strength curves provided by the CES 88-1 Proposed Specification using a factor of safety equal to unity. In using the proposed specification, the tangent modulus (E_t) was obtained from Table A13 and Fig. A11 of CES 88-1 for annealed columns of type 304 stainless steel, and the yield stress ($F_y = 28$ ksi $\simeq$193 MPa) was obtained from Table A1. As shown in Figs. 8a and 8b, the CES 88-1 Proposed Specification provides very conservative estimates of strength. In the low column slenderness range ($L_t/r < 40$), the CES 88-1 column strength is approximately half of the design strength provided by the design procedure proposed in Section 3.2. This difference reflects the strengthening effect of cold-working the tubes which is incorporated in the proposed design procedure. In the long column slenderness range, the influence of cold-work on the column strength becomes less important, and the difference between the column curves provided by the CES 88-1 and the proposed design procedure becomes less significant.

3.3.2 Factor of safety

The factor of safety (Ω) used for the design of columns in CES 88-1 is 2.15. This is made up from two components. Firstly a basic factor of safety of 1.92 is used in the American specifications for the allowable stress design of steel columns. Secondly, an additional factor of safety of 1.11 is applied to stainless steel sections due to the lack of design experience, and because in stainless steel design it is necessary to consider the inelastic behaviour at lower stresses than those used for carbon steel (Yu, 1985).

The basic factor of safety of 1.92 is higher than the factor of safety used in many other international standards for steel structures, including the Australian Steel Structures Standard (SAA 1981) for which the value is 1.67, since the American specifications are based on straight concentrically loaded column tests, whereas the Australian standards are based on eccentrically loaded column tests.

The test strengths of the eccentrically loaded columns included in this paper can be used to check the accuracy of design methods for stainless steel tubes which are based on the strength of imperfect columns. Such a method is calibrated for use in Australia in Rasmussen & Hancock (1990).

4 Conclusions

A test programme on stub columns and long columns of SHS and CHS stainless steel tubes has been performed. The stub column tests provided the stress-stain curves of the full cross-section from which the 0.2 % Proof Stresses and the tangent modulus versus stress curves could be deduced. The long column tests provided the reduction of column strength with increasing column length.

It was recommended that the SHS and CHS columns should be designed according to the Proposed Specification, 'Design of Cold-formed Stainless Steel Structural Members', (University of Missouri Rolla, Civil Engineering Study 88-1, 1988), except that,

- the tangent modulus should be determined using the stress-strain curves obtained from stub column tests of tubes in the cold-worked state, and
- the yield stress should be determined as the 0.2 % Proof Stress obtained from stub column tests, rather than from Table A1 of CES 88-1.

The proposed design procedure was compared with the tests using a factor of safety equal to unity. Generally, the design curves agreed well with the test strengths of the concentrically loaded columns, although the strengths were conservatively predicted in the short column length range. It was demonstrated that the proposed design procedure provided column strengths which were much closer to the test strengths than would have been the case if the CES 88-1 predictions, (based on the annealed properties), were used without modification.

5 Acknowledgement

The authors are grateful to BHP Coated Products Division - Stainless for permission to publish the test results and the proposed design method.

6 Appendix I. References

AISC (1986), Load and Resistance Factor Design Specification for Structural Steel Buildings, *American Institute of Steel Construction*, Chicago.

AISI (1968a), Specification for the Design of Light Gage Cold-formed Stainless Steel Members. *American Institute of Steel Construction*, New York.

AISI (1968b), Specification for the Design of Cold-formed Steel Structural Members. *American Institute of Steel Construction*, New York.

AISI (1974), Stainless Steel Cold-formed Structural Design Manual, *American Institute of Steel Construction*, New York.

AISI (1986), Specification for the Design of Cold-formed Steel Structural Members, Cold-formed Steel Design Manual, Part 1, *American Institute of Steel Construction*, New York.

Barlow, H.W., (1957), 'The Column Strength of Thin-walled Sections of 18-8 Stainless Steel', *American Society for Testing Materials*, Special Technical Publication No. 196.

Bild, S. & Trahair, N.S., (1988), 'Steel Column Strength Models', *Journal of Constructional Steel Research*, Vol. 11, No. 1.

Hill, H.N., (1944), 'Determination of Stress Strain Relations from the Offset Yield Strength Values', *NACA*, Technical Note No. 927.

Johnson, A.L., (1967), 'The Structural Performance of Austenitic Stainless Steel Members', *Cornell University Department of Structural Engineering Report No. 327*, Cornell University.

Johnson, A.L. & Winter, G., (1966), 'Behaviour of Stainless Steel Columns and Beams', *Journal of Structural Engineering, American Society of Civil Engineers*, Vol. 92, No. ST5.

Ramberg, W. & Osgood, W.R., (1943), 'Description of Stress Strain Curves by Three Parameters', *NACA*, Technical Note No. 902.

Rasmussen & Hancock (1990), 'Strength Tests on Stainless Steel Tubular Columns', *Proceedings*, Second National Structural Engineering Conference, Adelaide, Australia.

SAA (1974), Methods for Tensile Testing of Metals, AS1391-1974, *Standards Association of Australia*, Sydney.

SAA (1981), Steel Structures Code, AS1250-1981, *Standards Association of Australia*, Sydney.

University of Missouri-Rolla, (1988), 'Design of Cold-formed Stainless Steel Structural Members', Civil Engineering Study 88-1 (CES 88-1), Department of Civil Engineering, University of Missouri-Rolla.

Yu, W.-W., (1985), *Cold-Formed Steel Design*, John Wiley & sons, New York.

7 Appendix II: Notation

A	Cross-section area
B	Total width of SHS
d_o	Outer diameter of CHS
e_{01}, e_{02}	Eccentricities of applied load at end sections
E_t	Tangent modulus, $(d\sigma/d\varepsilon)$
E_0	Initial Young's Modulus
F_n	Flexural buckling stress
F_y	Yield stress
I	Second moment of area
L	Length of test specimen
L_b	Length of an end bearing
L_e	Effective column length

L_t	Column length (length between axes of pins in end bearings)
n	Exponent in Ramberg-Osgood formula
P_a	Flexural buckling load
P_u	Test strength
r	Radius of gyration
r_0	Corner radius of SHS
t	Plate thickness
v_{01}, v_{02}	Overall geometric imperfection at midlength
ε	Longitudinal strain
ε_u	Ultimate tensile strain
σ	Longitudinal stress
σ_{cr}	Critical stress for flexural buckling
σ_u	Ultimate tensile stress
$\sigma_{0.2}$	0.2 % Proof Stress
Ω	Factor of safety